Clin Orthop Relat Res (2012) 470:2431–2440
DOI 10.1007/s11999-012-2344-1

Clinical Orthopaedics and Related Research®
A Publication of The Association of Bone and Joint Surgeons®

SYMPOSIUM: LEGG-CALVÉ-PERTHES DISEASE: WHERE DO WE STAND AFTER 100 YEARS?

LCPD: Reduced Range of Motion Resulting From Extra- and Intraarticular Impingement

Moritz Tannast MD, Markus Hanke, Timo M. Ecker MD, Stephen B. Murphy MD, Christoph E. Albers MD, Marc Puls PhD

Published online: 11 April 2012

Abstract

Background Legg-Calvé-Perthes disease (LCPD) often results in a deformity that can be considered as a complex form of femoroacetabular impingement (FAI). Improved preoperative characterization of the FAI problem based on a noninvasive three-dimensional computer analysis may help to plan the appropriate operative treatment.

Questions/purposes We asked whether the location of impingement zones, the presence of additional extraarticular impingement, and the resulting ROM differ between hips with LCPD and normal hips or hips with FAI.

Methods We used a CT-based virtual dynamic motion analysis based on a motion algorithm to simulate the individual motion for 13 hips with LCPD, 22 hips with FAI, and 27 normal hips. We then determined the motion and impingement pattern of each hip for the anterior (flexion, adduction, internal rotation) and the posterior impingement tests (extension, adduction, external rotation).

Results The location of impingement zones in hips with LCPD differed compared with the FAI/normal groups. Intra- and extraarticular impingement was more frequent in LCPD (79% and 86%, respectively) compared with normal (15%, 15%) and FAI hips (36%, 14%). Hips with LCPD had decreased amplitude for all hip motions (flexion, extension, abduction, adduction, internal and external rotation) compared with FAI or normal.

Conclusions Hips with LCPD show a decreased ROM as a result of a higher prevalence of intra- and extraarticular FAI. Noninvasive assessment of impingement characteristics in hips with LCPD may be helpful in the future for establishment of a surgical plan.

Introduction

Legg-Calvé-Perthes disease (LCPD) is an idiopathic osteonecrosis of the capital femoral epiphysis in childhood that results in deformity of the proximal femur and acetabulum in 74% to 80% of all cases [10, 26]. The proximal femur typically presents with a mushroom-shaped aspherical femoral head, a short femoral neck, and a high-riding greater trochanter [26]. The acetabulum is involved secondarily and can be deficient and/or excessively covering [8, 26]. The deformity can be considered as a complex form of femoroacetabular impingement (FAI). The joint is often incongruent and acts more like a hinge rather than a ball and socket joint. The resulting motion consists of a complex interaction of rotation and translation. Differences in the location of the impinging anatomical structures and the resulting ROM may therefore substantially differ from idiopathic FAI.

Each author certifies that he or she, or a member of their immediate family, has no commercial associations (eg, consultancies, stock ownership, equity interest, patent/licensing arrangements, etc) that might pose a conflict of interest in connection with the submitted article.
All ICMJE Conflict of Interest Forms for authors and *Clinical Orthopaedics and Related Research* editors and board members are on file with the publication and can be viewed on request.
Each author certifies that his or her institution approved the human protocol for this investigation, that all investigations were conducted in conformity with ethical principles of research, and that informed consent for participation in the study was obtained.

M. Tannast (✉), M. Hanke, T. M. Ecker, C. E. Albers, M. Puls
Department of Orthopaedic Surgery, Inselspital, University of Bern, Freiburgsstrasse, 3010 Bern, Switzerland
e-mail: moritz.tannast@insel.ch

S. B. Murphy
Center for Computer Assisted and Reconstructive Surgery, New England Baptist Hospital, Tufts University School of Medicine, Boston, MA, USA

The aim of surgery in a painful hip with restricted motion and without advanced arthrosis after LCPD is to relieve all sources of FAI and thereby reduce pain and improve the ROM. Based on our experience with open surgical hip dislocation in these cases [9], conventional imaging modalities cannot always adequately visualize all sources of FAI. A better preoperative characterization of the impinging pathomorphologies may help the surgeon to plan the appropriate steps of operative treatment. This would help to ensure that all sources of impingement are addressed properly.

Noninvasive three-dimensional (3D) dynamic computer analysis has been used to characterize impingement sites in idiopathic FAI [14]. This method is based on a single rotation point, which is reasonably accurate for relatively spherical hips. Until recently, this method of 3D computer analysis has not provided reliable information on impingement sites in joints with marked asphericity of the femoral head such as in LCPD. The additional implementation of a novel algorithm (the equidistant method) now allows the virtual dynamic simulation of these nonconcentric joints [21–23]. This algorithm calculates ROM stepwise in 1° increments. For each step, the contact surfaces of the femur and the acetabulum are reconstructed. These surfaces are used to construct two best-fitting spheres (one femoral and one acetabular). To adjust for joint irregularities, the centers of rotation of these two spheres are then matched.

Using this novel algorithm, we can now noninvasively characterize sites of intra- and extraarticular impingement in LCPD and compare those characteristics with data from FAI and normal hips. This can provide clinically relevant information regarding the differences and similarities in hip motion between patients with LCPD, FAI, and normal hips. We therefore addressed the following questions: (1) how does the location of anterior and posterior FAI zones on the femur/acetabulum in hips with LCPD differ compared with normal and FAI hips; (2) does the prevalence of intra- and extraarticular impingement locations differ for LCPD hips in comparison to normal and FAI hips; and (3) how is ROM affected in hips with LCPD in comparison to normal hips and hips with FAI?

Patients and Methods

We performed a retrospective, computer-assisted comparative study of 56 subjects (62 hips). Three groups were evaluated: 11 patients with LCPD (13 hips), 26 normal subjects (27 hips), and 19 patients with FAI (22 hips). We recruited all patients from the outpatient clinic of one of the authors (SBM). The normal hips were selected from the contralateral hips of 146 patients undergoing CT-based computer-assisted THA. Hips with the following features were excluded: total hip or knee arthroplasty (n = 10), pain (n = 4), previous hip surgery (n = 3), osteoarthritis Grade 1 or higher according to Tönnis [32] (n = 40), lateral center-edge angle of less than 25° (n = 24), pistol grip deformity (n = 13) [26], coxa profunda (n = 13) [30], coxa vara or valga (n = 1), acetabular retroversion (n = 4) [24, 30], protrusio acetabuli (n = 2), alpha angle of more than 50° (n = 4) [18], and femoral retrotorsion (n = 1). The diagnosis of FAI for the FAI group was based on the current recommendations of a positive correlation among symptoms, findings during physical examination (pain in forced flexion, internal rotation, and adduction), and radiographic findings [30]. There were 13 hips with a combined cam-pincer type, six hips with a pure cam type, and three hips with a pure pincer-type impingement. Hips from the LCPD group were graded according to the Stulberg et al. classification [27]. The three study groups differed in terms of age, alpha angle, acetabular index, extrusion index, and femoral antetorsion (Table 1). The study was approved by the local institutional review board.

Based on the 3D information from a CT scan of the pelvis, we compared the computed ROM, the individual impingement zones, and the prevalence of intra- and extraarticular impingement among the three groups. For a minimal detectable difference of 22° of flexion [14], we calculated a minimum sample size of 12 hips for each group to provide a level of alpha of 0.01 and a beta of 0.10.

From all patients, a specific CT scan was available according to a previously defined protocol [14, 28]. The CT scan had to cover the entire pelvis as well as the proximal and the distal parts of the femur. Based on this CT scan, a 3D polygon model of the pelvis and the femur was built semiautomatically using the Amira Visualization Toolkit (Visage Imaging Inc, Carlsbad, CA, USA). We used a pelvic and a femoral coordinate system to define the neutral orientation of the hip. The pelvic coordinate system was the anterior pelvic plane, which was defined by the anterosuperior iliac spines and the pubic tubercles [29]. The femoral coordinate system was defined by the center of the femoral head, the knee center, and both femoral condyles. Femoral torsion was calculated according to Murphy et al. [17]. A least-squares spherical approximation to the points of the femoral head was used [16] to improve the accuracy of the determination of the femoral head center in LCPD hips. This method of a best-fitting sphere to determine the femoral head center in a nonspherical femoral head could be successfully used in a previous study [20]. Detection of this approximate femoral center is needed to initiate the algorithm and to objectify femoral torsion. This algorithm was then applied to compute the virtual simulation of the individual hip motion. This equidistant method [23] preserves a constant joint space by superimposing the

Table 1. Demographic and radiographic information of the three study groups

Parameter	LCPD	Normal	FAI	p value Overall	p value LCPD versus normal	p value LCPD versus FAI
Number of hips	13	27	22	–	–	–
Percentage of bilateral hips (percent bilateral)	15.4	3.7	13.6	0.731	0.242	0.774
Age (years)	41 ± 15 (22–69)	54 ± 11 (31–74)	36 ± 10 (17–49)	< 0.001	0.014	0.278
Gender (percent male of all hips)	77	56	68	0.377	0.169	0.440
Side (percent right of all hips)	31	33	50	0.395	0.584	0.226
Height (cm)	170 ± 8 (163–183)	168 ± 10 (158–195)	175 ± 7 (163–188)	0.065	0.609	0.148
Weight (kg)	75 ± 10 (63–93)	77 ± 16 (49–115)	80 ± 20 (52–127)	0.738	0.563	0.371
Body mass index (kg/m^2)	26 ± 3 (22–33)	27 ± 4 (20–36)	26 ± 5 (19–37)	0.641	0.441	0.997
Alpha angle (Nötzli)	128 ± 15 (111–162)	42 ± 5 (34–39)	62 ± 12 (40–84)	< 0.001	< 0.001	< 0.001
Lateral-edge angle (degrees)	28 ± 11 (8–45)	32 ± 5 (25–44)	33 ± 7 (17–42)	0.152	0.297	0.153
Centrum collum diaphyseal angle (degrees)	135 ± 10 (108–147)	130 ± 5 (122–140)	132 ± 7 (121–146)	0.165	0.164	0.517
Acetabular index (degrees)	15 ± 10 (4–32)	6 ± 4 (−6–13)	4 ± 5 (−10–14.2)	< 0.001	0.007	0.002
Extrusion index (percent)	32 ± 11.0 (15–50)	23 ± 5 (12–33)	18 ± 7.5 (4–35)	< 0.001	0.002	< 0.001
Femoral antetorsion (degrees)	35 ± 18 (−9–67)	21 ± 7 (7–39)	22 ± 8 (0–35)	0.001	0.021	0.036
Stulberg classification (%)		–	–	–	–	–
Grade 1	0					
Grade 2	0					
Grade 3	62					
Grade 4	23					
Grade 5	15					

Values are mean ± SD with ranges in parentheses; LCPD = Legg-Calvé-Perthes disease; FAI = femoroacetabular impingement.

articulating acetabular and femoral sphere centers. Based on a validated automatic rim detection procedure [22], the algorithm detects the articulating portion of the acetabulum and the corresponding area of the femoral head for each motion step. A best-fitting sphere is then calculated for both the acetabulum and the femoral head area. The center of both spheres is then automatically adjusted by the software for each motion step of 1°. This equidistant method is specifically designed for virtual analysis of more complex hip pathomorphologies (such as FAI and/or LCPD), validated, and was reportedly superior in terms of linear and angular accuracy to all other hip motion simulations [23]. The ROM can be predicted with an accuracy of 2.5°, FAI can be detected with a sensitivity of nearly 90% and a specificity of 75%, and the location of impingement can be determined with an accuracy of 1.2 mm [23]. This hip motion simulation could be successfully applied in a pilot study for LCPD [21]. Our software is unable to evaluate the stability of the joint.

Based on this computerized analysis, we calculated the ROM for the following motions for all three groups: flexion, extension, abduction, adduction, internal rotation, and external rotation (in 0° and 90° of flexion). In addition, two motion patterns were evaluated, which correspond to the anterior and the posterior impingement tests. For the anterior impingement test, internal rotation was studied in 5° increments between 60° and 130° of flexion and in 10° increments between –20° and 20° of adduction. Analogously for the posterior impingement test, external rotation was studied in 5° increments between 10° of flexion and 30° of extension and in 10° increments between –20° and 20° of adduction. For each of these patterns, the maximum impingement-free motion was calculated for each group.

The location of the impingement zones was quantified based on the sum and the distribution of all impingement points for every possible combination of motion for an individual patient. This resulted in 227 to 4201 impingement points per patient and was computed for the anterior and the posterior impingement tests separately. We then calculated the distribution of the impingement zones on the acetabulum and the femur using a clock system. Six o'clock was defined by the middle of the acetabular notch on the acetabular side and by the femoral axis on the femoral side, respectively. Three o'clock was consistently defined anteriorly both for right and left hips.

We then allocated the impingement zones to an anatomic location of the pelvis and the femur. The possible pelvic impingement areas were divided into: acetabular rim, intraarticular, supraacetabular, ischium, and anteroinferior iliac spine. The possible femoral impingement areas were divided into: femoral head, femoral neck, femoral head-neck junction, greater and lesser trochanter, intertrochanteric crest, and femoral shaft.

We confirmed normal distributions of continuous (amplitudes of ROM) data with the Kolmogorov-Smirnov test. We determined differences in ROM among the three study groups using the univariate analysis of variance. If significant, we used the unpaired t-test with adjustment for multiple comparison (Bonferroni correction) to compare two groups. To determine differences in location of impingement zones among the three study groups, the chi square test was used. To compare the location of FAI between two groups, the Fisher's exact test was performed. The same tests were used to determine differences in prevalence of intra- and extraarticular impingement.

Results

The anterior impingement zones on the acetabulum were located more anteroinferior in the LCPD group in comparison to the normal ($p < 0.001$) and the FAI groups ($p < 0.001$; Fig. 1A). The anterior impingement zones on the femur were located more inferiorly for the LCPD group in comparison to the normal ($p < 0.001$) and FAI groups ($p < 0.001$; Fig. 1B). The location of the posterior impingement zones on the acetabulum was more posterior for the LCPD group in comparison to the normal ($p < 0.001$) and the FAI groups ($p < 0.001$; Fig. 1C). The location of the posterior impingement zones on the femur was more posterior for the LCPD group in comparison to the normal group ($p < 0.001$) and the FAI group ($p < 0.001$; Fig. 1D).

We found a higher prevalence of extra- and intraarticular impingement for the anterior (Table 2) and the posterior impingement tests (Table 3) for the LCPD group in comparison to the normal and the FAI groups. For the anterior impingement test, LCPD hips had a higher prevalence of impingement for the femoral head, neck, head neck-junction, and shaft on the femoral side (Fig. 2A) and a higher prevalence of impingement for the rim on the acetabular side in comparison to the normal and the FAI groups (Fig. 2B). For the posterior impingement test, LCPD hips had a higher prevalence of impingement of the femoral head, neck, head-neck junction, lesser and greater trochanter, femoral shaft on the femoral side (Fig. 2C), and a higher prevalence of impingement of the rim, supraacetabular region, ischium, and the intraarticular compartment (p values; Fig. 2C–D).

Hips from the LCPD group had decreased amplitude for all evaluated hip motions (Table 4). For the anterior impingement test, internal rotation decreased with increasing flexion for the normal ($p < 0.001$) and the FAI ($p < 0.001$) groups, whereas it did not change for the LCPD group ($p = 0.989$; Fig. 3A). For the posterior impingement test, external rotation decreased with decreasing flexion for the normal ($p < 0.001$) and the FAI ($p < 0.001$) groups, whereas it did not change for the LCPD group ($p = 0.597$; Fig. 3B).

Discussion

Preoperative assessment of impingement sites with the resulting impairment of ROM of hips with LCPD is challenging because of their complex deformity. Location of the impingement zones and the presence of additional extraarticular impingement are hard to anticipate based on the clinical and the preoperative radiographic examinations. Understanding the pathologic motion and impingement sites in LCPD will help to establish a surgical plan. Based on a validated virtual three-dimensional dynamic analysis, we questioned (1) if the location of the impingement sites differs after LCPD in comparison to normal/FAI hips; (2) if hips after LCPD more frequently impinge intra- and extraarticularly; and (3) how this intra- and extraarticular FAI after LCPD affects ROM.

This study has limitations. First, the number of LCPD hips is too low to analyze the individual dynamic hip motion with respect to different Stulberg classes [27]. However, we were able to describe the motion pattern and the impingement pattern for hips with LCPD in general. Second, our analysis only shows the osseous impingement without taking into consideration the soft tissue structures. This explains for example the high external rotation in 90° of flexion for normal hips. Nevertheless, for the anterior and the posterior impingement motions, ROM is typically restricted by osseous landmarks [28] and we do not believe would compromise our findings and conclusions. With our method, the ROM is generally overestimated by approximately 2° [23] because the cartilage and the labrum are not integrated in the simulation. Third, our analysis does not allow us to simulate joint instability, which is not the major structural problem after LCPD [13]. Because only 23% of our LCPD hips had a steep acetabulum (Stulberg et al., Grade IV) without radiographic signs of subluxation (eg, broken Shenton's line), the presented results should be representative for the majority of hips after LCPD.

A number of studies report ROM after LCPD hips (Table 5). Zilkens et al. [33] report the clinical ROM after LCPD with similar results compared with our simulation. Most of the available literature deals with impairment of

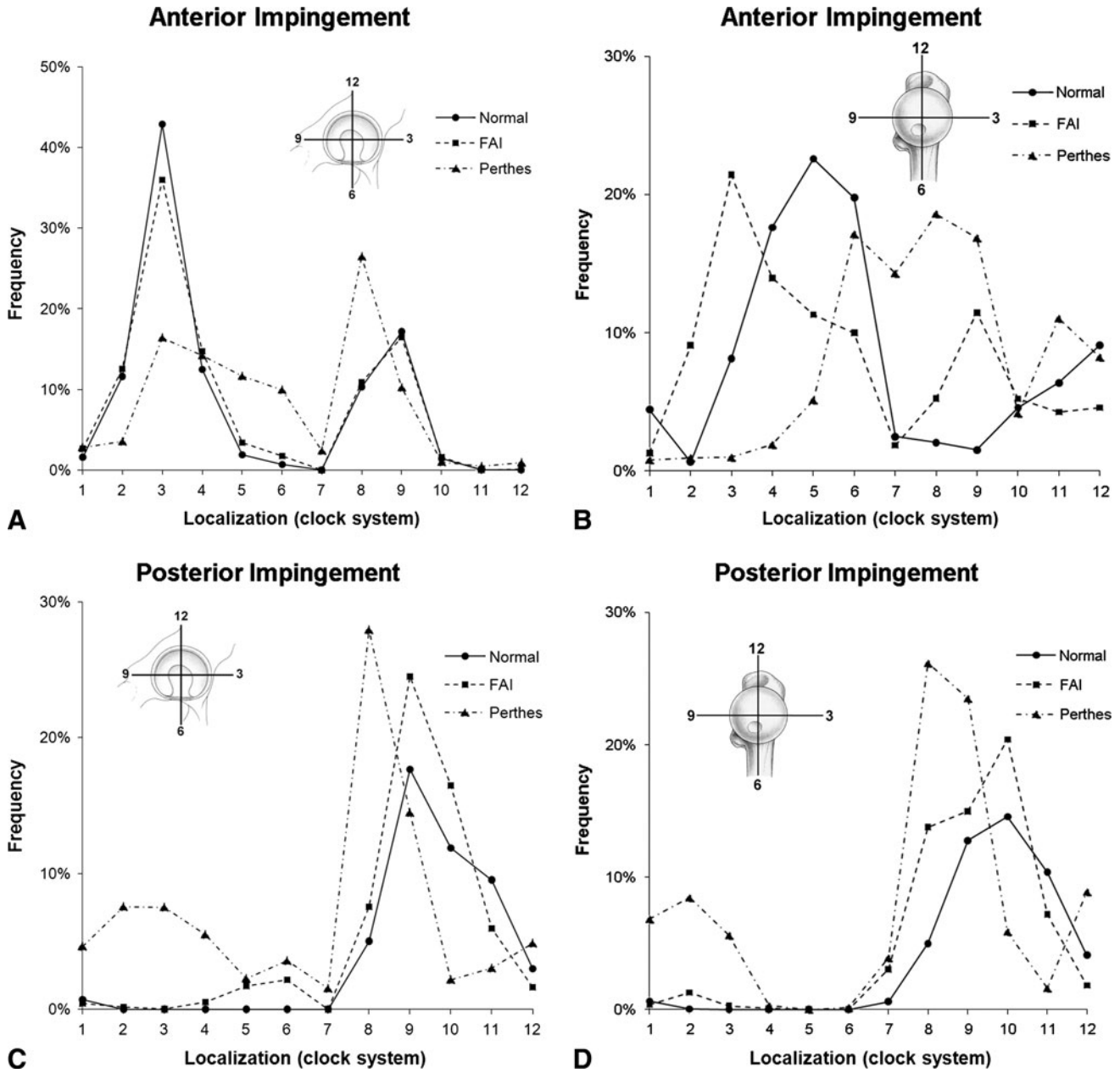

Fig. 1A–D The impingement zones of the anterior impingement test for the acetabular (**A**) and the femoral (**B**) side are shown. The impingement zones for the posterior impingement test for the acetabular (**C**) and the femoral sides (**D**) are shown.

hip motion amplitudes in childhood [25, 31]. Tayton [31] reported hip flexion of 136° in 51 children with LCPD. Rao et al. reported a similar value of approximately 130° flexion. This is even higher than the mean value of hip flexion in our normal group. An explanation for this discrepancy might be the unrecognized concomitant lumbar lordosis [14, 19, 28] and compensatory external rotation of the hip [7]. The only concise statement in terms of ROM refers to a limited rotation in flexion and/or extension and abduction [31]. Stanitski [25] reported no decreased ROM of hips in 78% of cases with LCPD when evaluated under anesthesia. The assumed cause for the predominantly limited abduction in the remaining 22% of cases was a soft tissue problem undergoing adductor tenotomy. However, based on our findings, this is more likely an intra- and/or extra-articular osseous impingement problem as described by Eijer et al. [9]. Our detected ROM in normal and FAI hips is comparable to other reports in the literature including clinical and computer-assisted results (Table 5). Hips with LCPD can be considered as severely impinging hips. This leads to an additional decrease of ROM compared with FAI and normal hips (Table 5).

Table 2. Prevalence of intra- and extraarticular impingement for the anterior impingement test*

Group	Acetabular		Femoral	
	Intraarticular	Extraarticular	Intraarticular	Extraarticular
LCPD	79%	79%	79%	86%
Normal	15%	15%	15%	15%
FAI	36%	9%	36%	14%
p value (overall)	< 0.001	< 0.001	< 0.001	< 0.001
p value (LCPD versus normal)	< 0.001	< 0.001	< 0.001	< 0.001
p value (LCPD versus FAI)	0.015	< 0.001	0.015	< 0.001

* Intraarticular acetabular zones were defined on the lunate surface and the acetabular rim (Fig. 2C). Extraarticular acetabular zones were defined on the ischium, near the anteroinferior iliac spine, and on the supraacetabular region (Fig. 2C). Intraarticular femoral zones were defined on the femoral head and the head-neck junction (Fig. 2A). Extraarticular femoral zones were defined on the greater or lesser trochanter, the lateral femoral neck, the intertrochanteric crest, or the femoral shaft (Fig. 2A–B); LCPD = Legg-Calvé-Perthes disease; FAI = femoroacetabular impingement.

Table 3. Prevalence of intra- and extraarticular impingement for the posterior impingement test*

Group	Acetabular		Femoral	
	Intraarticular	Extraarticular	Intraarticular	Extraarticular
LCPD	100%	100%	100%	57%
Normal	19%	11%	11%	11%
FAI	14%	9%	13%	5%
p value	< 0.001	< 0.001	< 0.001	< 0.001
p value (LCPD versus normal)	< 0.001	< 0.001	< 0.001	< 0.001
p value (LCPD versus FAI)	< 0.001	< 0.001	< 0.001	< 0.001

* Intraarticular acetabular zones were defined on the lunate surface and the acetabular rim (Fig. 2C). Extraarticular acetabular zones were defined on the ischium, near the anteroinferior iliac spine, and on the supraacetabular region (Fig. 2C). Intraarticular femoral zones were defined on the femoral head and the head-neck junction (Fig. 2A). Extraarticular femoral zones were defined on the greater or lesser trochanter, the lateral femoral neck, the intertrochanteric crest, or the femoral shaft (Fig. 2A–B); LCPD = Legg-Calvé-Perthes disease; FAI = femoroacetabular impingement.

The exact location of the impingement zones of LCPD hips has never been described in detail. It follows a characteristic pattern both for the anterior and the posterior impingement motion. In flexion and internal rotation, the deformed femoral head and neck leads to an intraarticular impingement between the anteroinferior aspherical portion of the femoral head and neck and the anterosuperior area of the acetabular rim in nearly all cases (Fig. 4A). This typically reduces internal rotation. In addition, there is often a pathologic extraarticular impingement that occurs between the greater trochanter and the supraacetabular area in abduction (if the femoral head-neck contour allows this; Fig. 4B). With pure hip flexion without abduction, the greater trochanter typically passes the supraacetabular area without collision, which still leads to relatively good hip flexion in LCPD. In extension and external rotation, the femoral head often collides with the posterior acetabular rim. In addition, extraarticular impingement of the lesser trochanter with the ischium and of the greater trochanter with the supraacetabular area is seen in approximately 50% of all cases (Fig. 4C).

The prevalence of extraarticular impingement in hips after LCPD is high. Once impingement is detected by clinical examination, it is not possible to accurately assess the location of impingement clinically. This might be the reason why this has never been reported in detail in the literature. For example, limited abduction could be the consequence of extraarticular impingement (between the greater trochanter and the pelvis) or the intraarticular impingement (between the flat femoral head and the acetabular rim). Particularly the extraarticular impingement of the lesser trochanter with the ischium is rarely described in the literature [12]. When performing joint-preserving surgery in hips after LCPD, every impingement source needs to be addressed. A repeated intraoperative assessment of the anterior and posterior impingement motions is mandatory after every surgical correction step to reveal additional sources of impingement. Our computerized analysis is an important

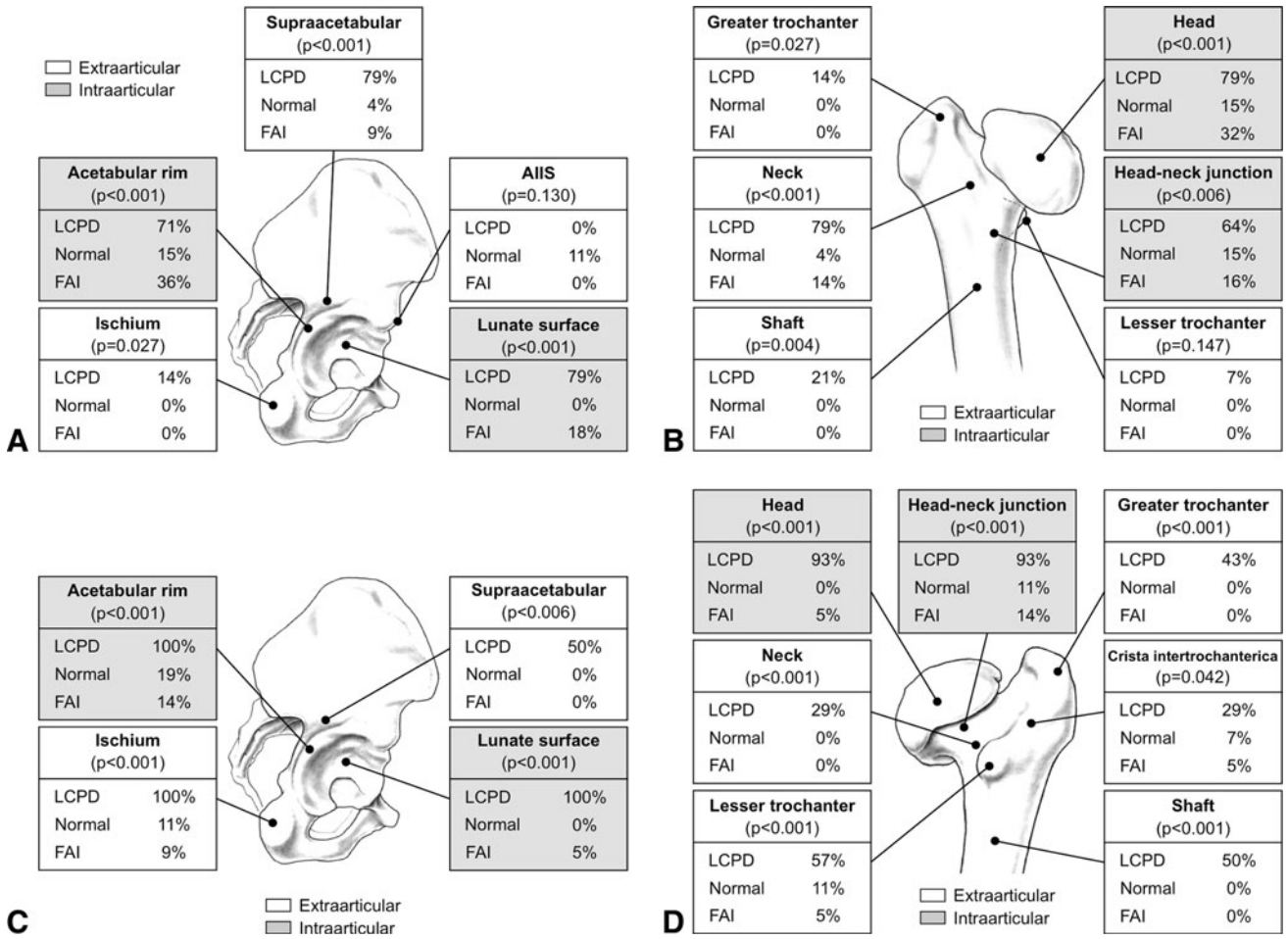

Fig. 2A–D The distribution of the impingement zones is shown for the anterior impingement test for the femoral (**A**) and the acetabular (**C**) side. Analogously, the distribution of the impingement zones for the posterior impingement test is shown for the femoral (**B**) and the acetabular sides (**D**). AIIS = anteroinferior iliac spine; LCPD = Legg-Calvé-Perthes disease; FAI = femoroacetabular impingement.

Table 4. Range of motion of control and study groups

Parameter	LCPD	Normal	FAI	p value Overall	p value LCPD versus normal	p value LCPD versus FAI
Flexion (degrees)	103 ± 40 (26–144)	125 ± 13 (103–146)	117 ± 14.4 (86–144)*	0.015	0.012	0.209
Extension	15 ± 27 (−39–50)	41 ± 8 (28–50)	33 ± 13 (19–44)	0.022	0.006	0.125
Abduction (degrees)	22 ± 23 (−18–78)	63 ± 12 (39–80)	56 ± 8 (40–69)	< 0.001	< 0.001	< 0.001
Adduction (degrees)	27 ± 15 (8–50)	38 ± 10 (13–58)	33 ± 9 (21–50)	0.009	0.031	0.199
Internal rotation in 0° of flexion (degrees)	24 ± 24 (−18–55)	110 ± 17 (84–146)	96 ± 20 (56–140)*	< 0.001	< 0.001	< 0.001
External rotation in 0° of flexion (degrees)	12 ± 34 (−51–76)	47 ± 12 (20–72)	43 ± 13 (18–68)	< 0.001	0.003	0.007
Internal rotation in 90° of flexion (degrees)*	−5 ± 23 (−40–40)	33 ± 9 (13–40)	21 ± 15 (−8–40)*	< 0.001	< 0.001	0.009
External rotation in 90° of flexion	59 ± 35 (14–140)	103 ± 13 (74–128)	99 ± 19 (45–125)	< 0.001	< 0.001	0.006

* Values calculated for hips with a minimum of 90° of flexion only. Values are expressed as mean ± SD with range in parentheses; LCPD = Legg-Calvé-Perthes disease; FAI = femoroacetabular impingement.

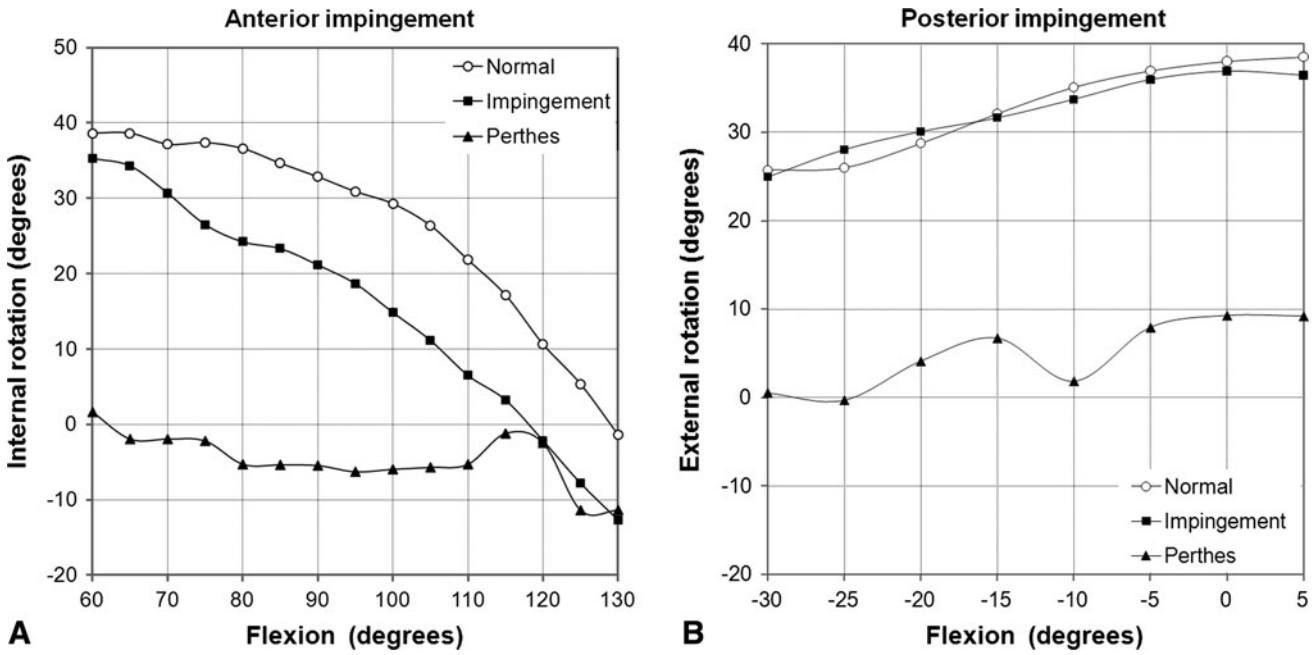

Fig. 3A–B The graph shows the ROM pattern for the three study groups for the anterior and posterior impingement test motion in 0° adduction/abduction. (**A**) Results of the motion pattern for the anterior impingement test. Internal rotation decreased for the normal and the FAI groups, whereas it did not change for the LCPD group. (**B**) Results of the motion pattern for the posterior impingement test. External rotation decreased with increasing extension for the normal and the FAI group, whereas it did not change for the LCPD group.

Table 5. Selected publications for hip range of motion in the literature

Author	Group	Method	Flexion (degrees)*	Internal rotation (degrees)*
Greene [11]	Normal	Clinical	120 ± 8	33 ± 8
Brunner et al. [5]	Normal	Clinical	119	36
Ahlberg et al. [1]	Normal	Clinical	131 ± 14	37 ± 12
Boone and Azen [4]	Normal	Clinical	122 ± 6	47 ± 6
Kubiak-Langer et al. [14]	Normal	Computer model	122 ± 16	35 + 6
Nussbaumer et al. [19]	Normal	Clinical	112 ± 11	34 ± 10
Tannast et al. [28]	Normal	Computer model	121 ± 12	35 ± 12
Audenaert et al. [2]	FAI	Computer model	110 ± 7	19 ± 6
Bedi et al. [3]	FAI	Computer model	107 ± 12	19 ± 13
Clohisy et al. [6]	FAI	Clinical	97 ± 9	9 ± 8
Kubiak-Langer et al. [14]	FAI	Computer model	105 ± 12	11 ± 7
Nussbaumer et al. [19]	FAI	Clinical	103 ± 16	26 ± 11
Tannast et al. [28]	FAI	Computer model	105 ± 16	11 ± 7
Lincoln et al. [15]	FAI	Clinical	94 ± 3	7 ± 2
Brunner et al. [5]	FAI	Clinical	111	8
Zilkens et al. [33]	LCPD	Clinical	107 ± 10	22 ± 14
Tannast et al. (present study)	LCPD	Computer model	100 ± 40	−5 ± 23

* Mean ± SD; FAI = femoroacetabular impingement; LCPD = Legg-Calvé-Perthes disease.

adjunct for the preoperative evaluation of patients with LCPD and planning of consequent joint-preserving surgery.

In summary, the dynamic motion pattern differs between hips with LCPD and normal hips or hips with FAI. Decreased ROM, a more extensive acetabular and femoral

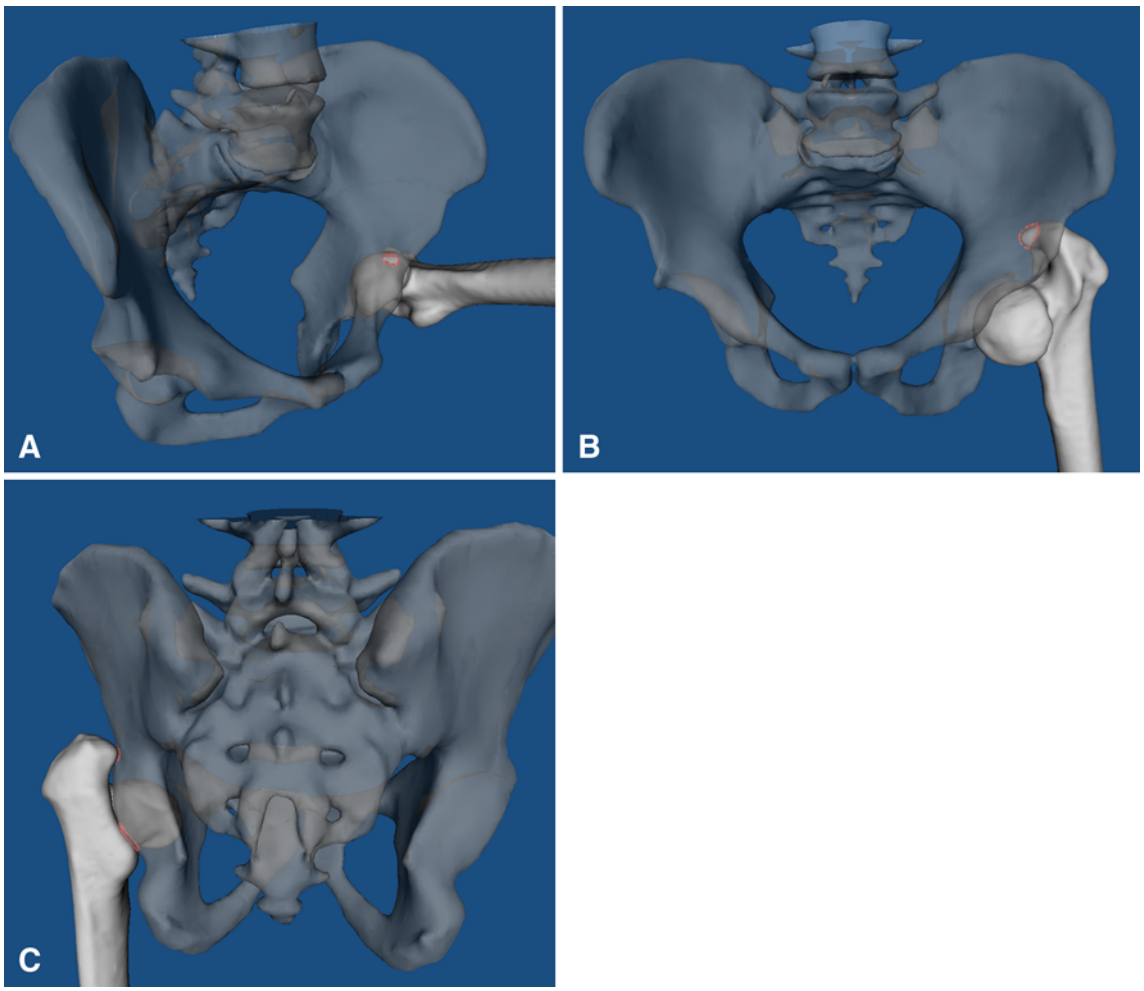

Fig. 4A–C (**A**) In deep flexion, a typical impingement is seen in LCPD between the anteroinferior portion of the femoral head and the anterosuperior area of the acetabulum. (**B**) Hip abduction typically leads to a supraacetabular extraarticular impingement with the greater trochanter. (**C**) Extension and external rotation reveals the extraarticular impingement posteriorly of the area of both trochanters with the posterior column area.

impingement zone, and a higher prevalence of extraarticular impingement are typical for LCPD. Noninvasive dynamic assessment of the FAI conflict in hips after LCPD may be helpful in future for establishment of a surgical plan.

References

1. Ahlberg A, Moussa M, Al-Nahdi M. On geographical variations in the normal range of joint motion. *Clin Orthop Relat Res.* 1988;234:229–231.
2. Audenaert EA, Mahieu P, Pattyn C. Three-dimensional assessment of cam engagement in femoroacetabular impingement. *Arthroscopy.* 2011;27:167–171.
3. Bedi A, Dolan M, Hetsroni I, Magennis E, Lipman J, Buly R, Kelly BT. Surgical treatment of femoroacetabular impingement improves hip kinematics: a computer-assisted model. *Am J Sports Med.* 2011;39(Suppl):43S–49S.
4. Boone DC, Azen SP. Normal range of motion of joints in male subjects. *J Bone Joint Surg Am.* 1979;61:756–759.
5. Brunner A, Hamers AT, Fitze M, Herzog RF. The plain beta-angle measured on radiographs in the assessment of femoroacetabular impingement. *J Bone Joint Surg Br.* 2010;92:1203–1208.
6. Clohisy JC, Knaus ER, Hunt DM, Lesher JM, Harris-Hayes M, Prather H. Clinical presentation of patients with symptomatic anterior hip impingement. *Clin Orthop Relat Res.* 2009;467:638–644.
7. Drehmann F. [Drehmann's sign. A clinical examination method in epiphysiolysis (slipping of the upper femoral epiphysis). Description of signs, aetiopathogenetic considerations, clinical experience (author's transl)]. *Z Orthop Ihre Grenzgeb.* 1979;117:333–344.
8. Eijer H, Berg RP, Haverkamp D, Pecasse GA. Hip deformity in symptomatic adult Perthes' disease. *Acta Orthop Belg.* 2006;72:683–692.
9. Eijer H, Podeszwa DA, Ganz R, Leunig M. Evaluation and treatment of young adults with femoro-acetabular impingement secondary to Perthes' disease. *Hip Int.* 2006;16:273–280.

10. Froberg L, Christensen F, Pedersen NW, Overgaard S. Long-term follow-up of a patient cohort with Legg-Calve-Perthes disease. *J Pediatr Orthop B.* 2011;20:273–277.
11. Greene WB. The clinical measurement of joint motion. In: Greene WB, Heckman JD, eds. *The Hip.* Rosemont, IL, USA: American Academy of Orthopaedic Surgeons; 1994:99–114.
12. Johnson KA. Impingement of the lesser trochanter on the ischial ramus after total hip arthroplasty. Report of three cases. *J Bone Joint Surg Am.* 1977;59:268–269.
13. Kim YJ, Novais EN. Diagnosis and treatment of femoroacetabular impingement in Legg-Calve-Perthes disease. *J Pediatr Orthop.* 2011;31:S235–S240.
14. Kubiak-Langer M, Tannast M, Murphy SB, Siebenrock KA, Langlotz F. Range of motion in anterior femoroacetabular impingement. *Clin Orthop Relat Res.* 2007;458:117–124.
15. Lincoln M, Johnston K, Muldoon M, Santore R. Combined arthroscopic and modified open approach for cam femoroacetabular impingement: a preliminary experience. *Arthroscopy.* 2009;25:392–399.
16. Mahaisavariya B, Sitthiseripratip K, Tongdee T, Bohez EL, Vander Sloten J, Oris P. Morphological study of the proximal femur: a new method of geometrical assessment using 3-dimensional reverse engineering. *Med Eng Phys.* 2002;24:617–622.
17. Murphy SB, Simon SR, Kijewski PK, Wilkinson RH, Griscom NT. Femoral anteversion. *J Bone Joint Surg Am.* 1987;69: 1169–1176.
18. Notzli HP, Wyss TF, Stoecklin CH, Schmid MR, Treiber K, Hodler J. The contour of the femoral head-neck junction as a predictor for the risk of anterior impingement. *J Bone Joint Surg Br.* 2002;84:556–560.
19. Nussbaumer S, Leunig M, Glatthorn JF, Stauffacher S, Gerber H, Maffiuletti NA. Validity and test-retest reliability of manual goniometers for measuring passive hip range of motion in femoroacetabular impingement patients. *BMC Musculoskelet Disord.* 2010;11:194.
20. Pienkowski D, Resig J, Talwalkar V, Tylkowski C. Novel three-dimensional MRI technique for study of cartilaginous hip surfaces in Legg-Calve-Perthes disease. *J Orthop Res.* 2009;27: 981–988.
21. Puls M, Ecker TM, Steppacher SD, Murphy SB, Kowal JH, Siebenrock KA, Tannast M. Prediction of impingement-free motion in Legg-Calvé-Perthes disease—an experimental pilot study. In: Davies BL, Joskowicz L, Murphy SB, eds. *Computer Assisted Orthopaedic Surgery*. Berlin, Germany: Pro Business; 2009:323–325.
22. Puls M, Ecker TM, Steppacher SD, Tannast M, Siebenrock KA, Kowal JH. Automated detection of the osseous acetabular rim using three-dimensional models of the pelvis. *Comput Biol Med.* 2011;41:285–291.
23. Puls M, Ecker TM, Tannast M, Steppacher SD, Siebenrock KA, Kowal JH. The Equidistant Method—a novel hip joint simulation algorithm for detection of femoroacetabular impingement. *Comput Aided Surg.* 2010;15:75–82.
24. Reynolds D, Lucas J, Klaue K. Retroversion of the acetabulum. A cause of hip pain. *J Bone Joint Surg Br.* 1999;81:281–288.
25. Stanitski CL. Hip range of motion in Perthes' disease: comparison of pre-operative and intra-operative values. *J Child Orthop.* 2007;1:33–35.
26. Stulberg SD. Unrecognized childhood hip disease: a major cause of idiopathic osteoarthritis of the hip. In: Cordell LD, Harris WH, Ramsey PL. *The Hip: Proc 3rd Meeting of The Hip Society.* St Louis, MO, USA: CV Mosby; New York, NY, USA: Springer; 1975:212–228.
27. Stulberg SD, Cooperman DR, Wallensten R. The natural history of Legg-Calve-Perthes disease. *J Bone Joint Surg Am.* 1981;63: 1095–1108.
28. Tannast M, Kubiak-Langer M, Langlotz F, Puls M, Murphy SB, Siebenrock KA. Noninvasive three-dimensional assessment of femoroacetabular impingement. *J Orthop Res.* 2007;25:122–131.
29. Tannast M, Langlotz U, Siebenrock KA, Wiese M, Bernsmann K, Langlotz F. Anatomic referencing of cup orientation in total hip arthroplasty. *Clin Orthop Relat Res.* 2005;436:144–150.
30. Tannast M, Siebenrock KA, Anderson SE. Femoroacetabular impingement: radiographic diagnosis-what the radiologist should know. *AJR Am J Roentgenol.* 2007;188:1540–1552.
31. Tayton K. The genesis of Perthes' disease: does it lie in hips with reduced ranges of movement? *J Pediatr Orthop B.* 2010;19: 327–332.
32. Tönnis D. Gerneral radiography of the hip joint. In: Tönnis D, ed. *Congenital Dysplasia, Dislocation of the Hip.* New York, NY, USA: Springer; 1987:100–142.
33. Zilkens C, Bittersohl B, Jager M, Haamberg T, Westhoff B, Krauspe R. Clinical presentation of young adults after Legg-Calve-Perthes disease. *Acta Orthop Belg.* 2009;75:754–760.